Investigation of the C–Cl Bonds in Trichloroacrylic Acid, $Cl_2C=CClCOOH$, by Single Crystal Zeeman Split NQR *

Gary Wulfsberg[a], Norbert Weiden[b], and Alarich Weiss[b]

[a] Department of Chemistry and Physics, Middle Tennessee State University, Murfreesboro, Tennessee 37132, USA
[b] Institut für Physikalische Chemie, Technische Hochschule Darmstadt, Petersenstr. 20, D-6100 Darmstadt, West Germany

Z. Naturforsch. **45a**, 243–248 (1990); received August 21, 1989

The ^{35}Cl NQR spectrum of trichloroacrylic acid, $Cl_2C=CClCOOH$, was studied by single crystal Zeeman NQR spectroscopy at 303 K (high temperature phase I) and at 275 K (low temperature phase II). At 303 K for the $=CCl_2$ group chlorines it was found $eQ\Phi_{zz}h^{-1}(^{35}Cl^{(2)}) = 76.179$ MHz, $\eta(^{35}Cl) = 0.1597$; $eQ\Phi_{zz}h^{-1}(^{35}Cl^{(3)}) = 74.693$ MHz, $\eta(^{35}Cl) = 0.1868$ and for the $=CClC-$ group chlorine $eQ\Phi_{zz}h^{-1}(^{35}Cl^{(1)}) = 75.145$ MHz, $\eta(^{35}Cl) = 0.1568$. The difference in the electric field gradients at the stereochemically inequivalent chlorines $Cl^{(2)}$ and $Cl^{(3)}$ is rather large. The asymmetry parameter $\eta(^{35}Cl^{(1)})$ shows an unusual temperature dependence which probably originates from the change of the hydrogen dynamics and position within the dimeric H-bonded unit $(Cl_2C=CClCOOH)_2$ during the phase transition.

Introduction

Recently we have observed a phase transition of trichloroacrylic acid, $Cl_2C=CClCOOH$, which occurs at $T_c = 292.5$ K. T_c is very sensitive to deuteration, and T_c of the deuterated compound, $Cl_2=CClCOOD$, is found almost ten degrees lower, at 283.7 K. The phase transition is easily observed by differential thermal analysis, DTA; the enthalpy of transition ΔH_{tr} was estimated to $\approx 250\ J \cdot mol^{-1}$. The crystal structure determination of the high temperature phase I of the protonated compound at 297 K has shown that this phase crystallizes with the centrosymmetric, monoclinic space group $C_{2h}^5 - P2_1/c$, and $Z = 4$. The low temperature Phase II is assumed to be non-centrosymmetric because pyroelectricity was observed at $T < T_c$. The pyroelectric coefficient at constant stress x, $p^{(x)}$, is very small, $p^{(x)} \approx 0.015\ \mu C\ m^{-2}\ K^{-1}$ at 270 K, raising to $\approx 0.10\ \mu C\ m^{-2}\ K^{-1}$ at its maximum near T_c. The dielectric constant ε is increasing near T_c by a factor of ≈ 1.5. Finally, ^{35}Cl NQR experiments on polycrystalline samples show a very slight change in $d\nu(^{35}Cl)/dT$ at T_c for both, the protonated and the deuterated compound [1].

The crystal structure suggests that the phase transition must be connected with the hydrogen (deuterium) position in the solid, which is composed of dimer units.

To gain more information on the solid state properties of trichloroacrylic acid, we performed single crystal Zeeman-splitting ^{35}Cl NQR experiments above and below T_c.

Experimental

Large single crystals of $Cl_2C=CClCOOH$, grown from the solution [1], were available. A suitable example was enclosed in a test tube (the vapor pressure of trichloroacrylic acid is quite high at room temperature), fixed on a goniometer head, adjusted optically, and transferred to the 4 π-Zeeman NQR goniometer [2]. The desired temperature of the crystal was maintained by a stream of flow and temperature regulated N_2-gas. The measurements of the sample temperature were accurate to ± 0.5 K. A pulsed NQR spectrometer was used in connection with the 4 π-Zeeman goniometer to measure the Zeeman split ^{35}Cl NQR spectra and to locate the zero splitting cones [3]. Because of the great linewidth of about 40 kHz of the ^{35}Cl resonance lines a pulse echo technique rather than Fourier transformation (FT) of the free induction decay has been applied. To locate the zero splitting positions two methods have been used: i) Monitoring of the echo height as a function of the orientation of

* Presented at the Xth International Symposium on Nuclear Quadrupole Resonance Spectroscopy, Takayama, Japan, August 22–26, 1989.

Reprint requests to Prof. Dr. Al. Weiss, Institut für Physikalische Chemie, Technische Hochschule Darmstadt, Petersenstraße 20, D-6100 Darmstadt.

0932-0784 / 90 / 0300-0243 $ 01.30/0. – Please order a reprint rather than making your own copy.

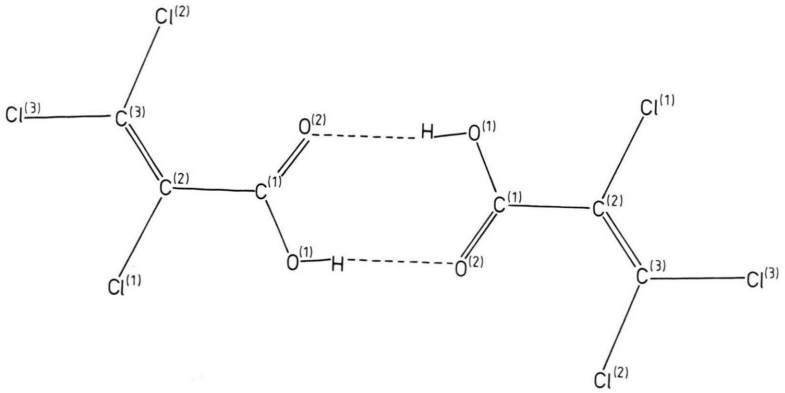

Fig. 1. Sketch of the dimeric, hydrogen bonded unit $(Cl_2C=CClCOOH)_2$.

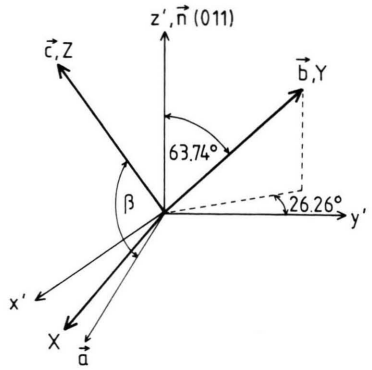

Fig. 2. Coordinate systems, used throughout this paper, X, Y, Z is the orthogonal crystal axes system with $Y \parallel b$, $Z \parallel c$, and $< (X, \alpha) = \beta - 90°$. x', y', z' is the orthogonal system of the Helmholtz coils (laboratory coordinate system). The crystal has been oriented with $\boldsymbol{n}\,(011) \parallel z'$.

Table 1. Asymmetry parameters $\eta\,(^{35}Cl)$, NQR frequencies, $\nu\,(^{35}Cl)$, and nuclear quadrupole coupling constants $eQ\Phi_{zz}h^{-1}\,(^{35}Cl)$ in trichloroacrylic acid at $T=275$ K and $T=303$ K.

Atom	T/K	$\eta\,(^{35}Cl)$	$\nu\,(^{35}Cl)$/ MHz	$eQ\Phi_{zz}h^{-1}\,(^{35}Cl)$/ MHz
$Cl^{(1)}$	275	0.1509	37.870	75.454
$Cl^{(1)}$	303	0.1568	37.726	75.145
$Cl^{(2)}$	275	0.1642	38.415	76.487
$Cl^{(2)}$	303	0.1597	38.251	76.179
$Cl^{(3)}$	275	0.1705	37.645	74.928
$Cl^{(3)}$	303	0.1686	37.523	74.693

the magnetic field with respect to the crystal with a boxcar. ii) Acquisition of about 1000 echos followed by FT of half of the echo. Method i) is by far faster than method ii), which is more accurate since both the maximum of the signal intensity and the minimum of the linewidth are obtained. So method i) has been used to locate the zero splitting cones and method ii) to refine them. Zeeman fields up to $350 \cdot 10^{-4}$ T were applied. Up to 40 zero splitting positions (ϑ, ϕ) were used for each cone to determine by a least squares procedure the nuclear quadrupole coupling constants $eQ\Phi_{zz}h^{-1}\,(^{35}Cl)$, the asymmetry parameters $\eta\,(^{35}Cl)$, and the direction cosines of the electric field gradient tensors, EFGT, at the chlorine sites. In Fig. 2 the coordinate system used throughout this paper is shown.

Results

In Figs. 3–5 the zero splitting cones found at $T=275$ K and 303 K are shown in a (ϑ, ϕ)-diagram. Within the accuracy of the drawings no differences in the zero splitting cones for the two temperatures can be seen. The angles ϑ and ϕ refer to the coordinate system x', y', z' of Figure 2. Table 1 gives the final results gained thereform, that is $\nu\,(^{35}Cl)$ (which are in agreement with the reported ones [1]), $eQ\Phi_{zz}h^{-1}\,(^{35}Cl)$, and $\eta\,(^{35}Cl)$. e is the protonic charge, Q the nuclear electric quadrupole moment of ^{35}Cl, and $\Phi_{zz}=eq$ the main principal value of the EFGT. $\eta\,(^{35}Cl)$ is defined by the principal axes system of the EFGT, Φ_{xx}, Φ_{yy}, Φ_{zz}. The relevant relations are

$$|\Phi_{xx}| \leqq |\Phi_{yy}| \leqq |\Phi_{zz}|, \quad \Phi_{xx}+\Phi_{yy}+\Phi_{zz}=0, \qquad (1)$$

$$\eta=(\Phi_{xx}-\Phi_{yy})/\Phi_{zz}.$$

In Table 2a the direction cosines of the principal EFGT-axes with respect to the orthogonal crystal axes system X, Y, Z are listed for $T=275$ K, and in Table 2b the direction cosines for $T=303$ K. In this Table the direction cosines of the bonds C–Cl are included, too.

Discussion

Considering the crystal structure of phase I of $Cl_2C=CClCOOH$, the dimeric units are formed by H-bonds, with a bond distance $O-H\cdots O$ of 267.7 pm. This distance is well within the range one finds for unsymmetric H-bonds $-O-H\cdots O$ in solids. In Fig. 6 we show the projection of the crystal structure of phase I onto the $(b\,c)$-plane. A calculation of the best plane through the three chlorine atoms and

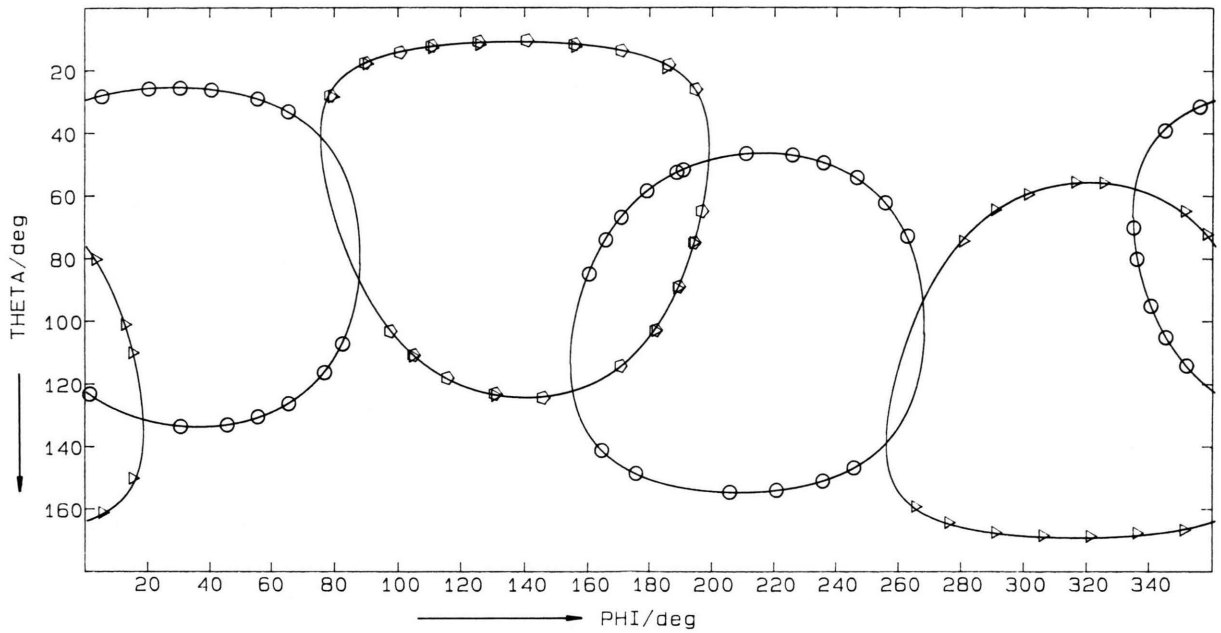

Fig. 3. ^{35}Cl NQR zero splitting cones of $Cl^{(1)} = \nu_2$ in trichloroacrylic acid. ○, ◇: symmetry related cones at 275 K; △: zero splitting cone position (ϑ, ϕ) at 303 K. The numbering of the frequencies is: ν_1 (^{35}Cl) is the highest frequency at 297 K, ν_3 (^{35}Cl) is the lowest one [1].

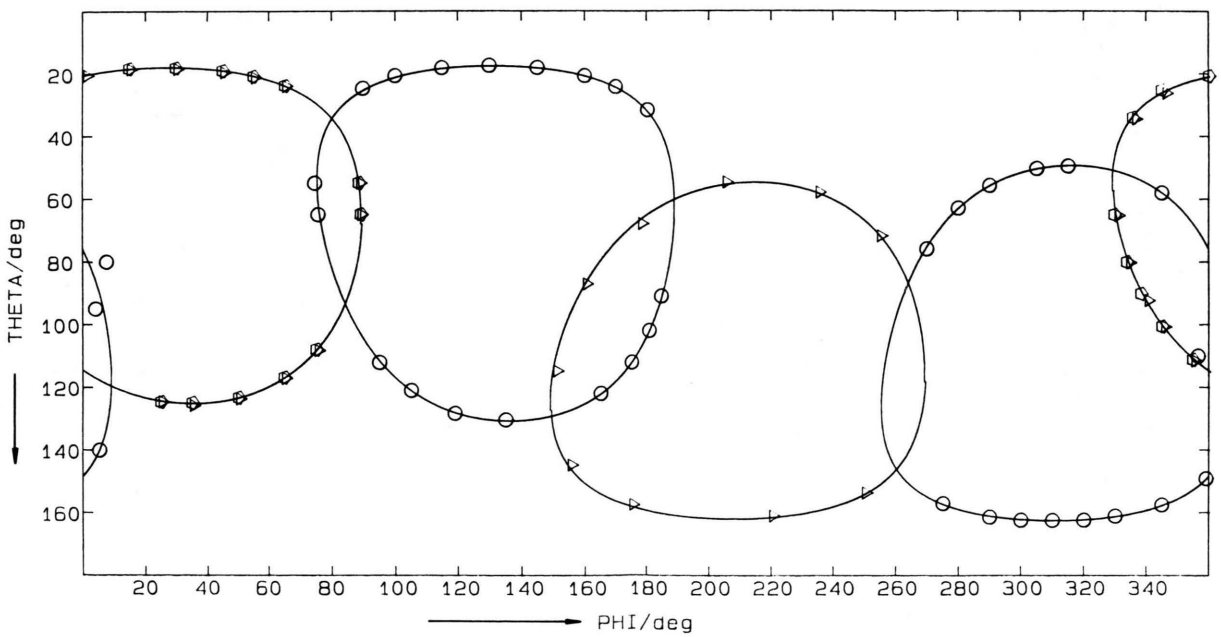

Fig. 4. ^{35}Cl NQR zero splitting cones of $Cl^{(2)} = \nu_1$ in trichloroacrylic acid. ○, ◇: symmetry related cones at 275 K; △: zero splitting cone position (ϑ, ϕ) at 303 K.

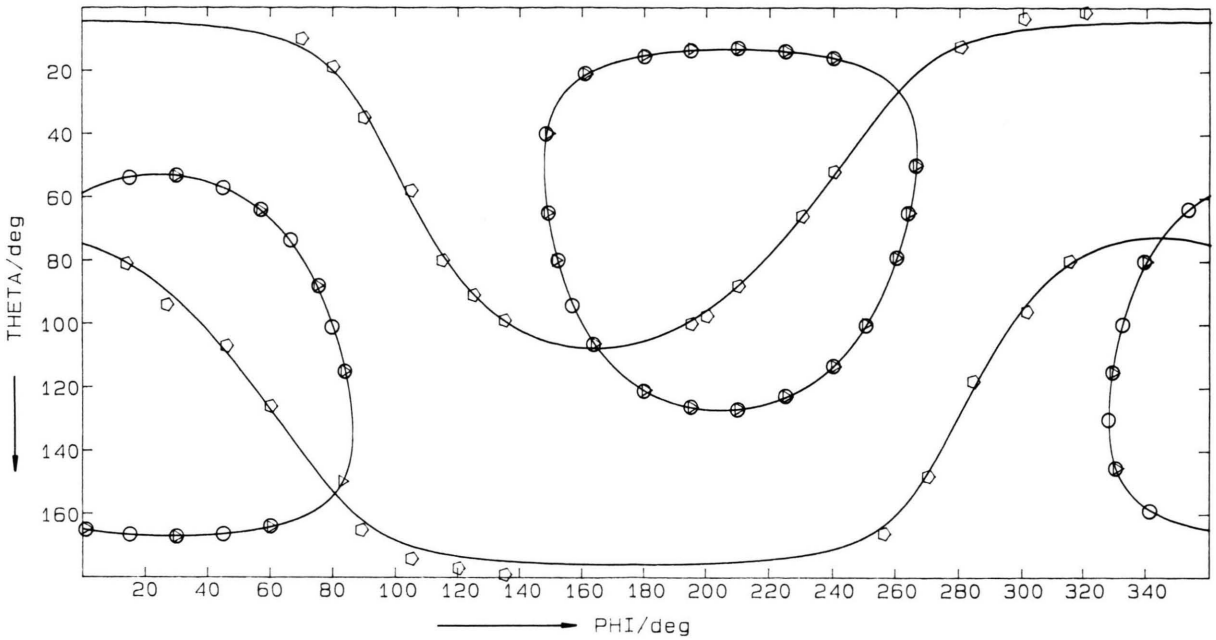

Fig. 5. ^{35}Cl NQR zero splitting cones of $Cl^{(3)} = \nu_3$ in trichloroacrylic acid. o, ◇: symmetry related cones at 275 K; △: zero splitting cone position (ϑ, ϕ) at 303 K.

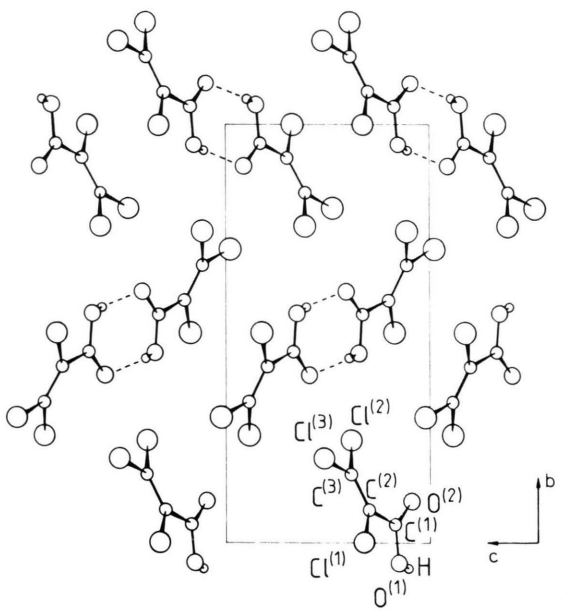

Fig. 6. Projection of the crystal structure of trichloroacrylic acid along [100] onto the plane (*b c*).

the three carbon atoms of the molecule shows strong planarity with a maximum deviation of 5 pm for these 6 atoms. The best plane through the carboxyl group CO_2 is slightly rotated against the C_3Cl_3-skeleton. In Table 3 the best planes and the deviations of the atoms from it are listed. Since the dimeric unit is formed by two molecules which are at different heigths with respect to the crystal axis ***a***, the planes of both skeletons C_3Cl_3 belonging to one dimeric unit are parallel, but with slightly different distances from the origin of the unit cell (139 pm and 149 pm).

The ^{35}Cl NQR measurements show very little change due to the phase transition at T_c [1]. To make a comparison of the crystal structure and the Zeeman-NQR data possible, we have linearly interpolated from the measurements at 303 K and 275 K $\eta(^{35}Cl)$ and $eQ\Phi_{zz}h^{-1}(^{35}Cl)$ at 297 K. The corresponding resonance frequencies have been calculated with the help of the polynomials given in [1].

In Table 4 the resulting values are found, together with the corresponding bond lengths C–Cl. The angles of the directions of Φ_{ii}, $i = x, y, z$, with respect to the structure and orientation of the molecules $Cl_2C=CClCOOH$ are listed in Table 5.

In first approximation, the orientation of the ^{35}Cl EFGT's follows the rule: Φ_{zz} is parallel to the corresponding bond $C-Cl^{(j)}$ and Φ_{xx} is parallel to the normal ***n*** of the plane ($Cl^{(3)}$ $C^{(2)}$ $C^{(1)}$). In Fig. 7 the molecule $Cl_2C=CClCOOH$ is sketched in a projection parallel to the skeleton $C^{(1)}$ $C^{(2)}$ $C^{(3)}$. The strong planarity of the plane ($C^{(1)}$ $C^{(2)}$ $C^{(3)}$ $Cl^{(1)}$ $Cl^{(2)}$ $Cl^{(3)}$) shows up clearly. The small differences between bond

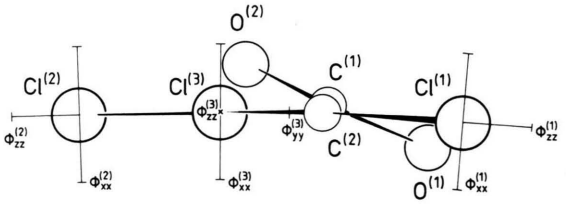

Fig. 7. Projection of the molecule $Cl_2C=CClCOOH$ parallel to the plane $(C^{(1)}\,C^{(2)}\,C^{(3)})$.

Table 2a. Direction cosines of the principal axes Φ_{xx}, Φ_{yy}, and Φ_{zz} of the electric field gradient tensors at 275 K with the orthogonal crystal axes system X, Y, Z (see Figure 1). The direction cosines for the atom $Cl^{(j)}$ are defined as $\lambda^{(j)}=\cos(\Phi_{xx}^{(j)}, X)\ldots\nu^{(j)}=\cos(\Phi_{zz}^{(j)}, Z)$.

Atom	$\Phi_{ii}^{(j)}$	$\lambda^{(j)}$	$\mu^{(j)}$	$\nu^{(j)}$
$Cl^{(1)}$	$\Phi_{xx}^{(1)}$	−0.10006	−0.36921	+0.92394
	$\Phi_{yy}^{(1)}$	−0.65503	−0.67452	−0.34049
	$\Phi_{zz}^{(1)}$	+0.74893	−0.63928	−0.17453
$Cl^{(2)}$	$\Phi_{xx}^{(2)}$	−0.09705	−0.48139	+0.87111
	$\Phi_{yy}^{(2)}$	+0.72097	+0.56937	+0.39497
	$\Phi_{zz}^{(2)}$	−0.68612	+0.66638	+0.29182
$Cl^{(3)}$	$\Phi_{xx}^{(3)}$	−0.04998	−0.45052	+0.89136
	$\Phi_{yy}^{(3)}$	+0.37703	−0.83497	−0.40088
	$\Phi_{zz}^{(3)}$	+0.92485	+0.31600	+0.21159

Table 2b. Direction cosines of the principal axes of the electric field gradient tensors at 303 K and of the bond directions $C^{(i)}-Cl^{(j)}$, $i=1,2,j=1,2,3$, with the orthogonal crystal axes system.

Atom	$\Phi_{ii}^{(j)}$	$\lambda^{(j)}$	$\mu^{(j)}$	$\nu^{(j)}$
$Cl^{(1)}$	$\Phi_{xx}^{(1)}$	−0.09879	−0.37974	+0.91980
	$\Phi_{yy}^{(1)}$	−0.65609	−0.67012	−0.34712
	$\Phi_{zz}^{(1)}$	+0.74818	−0.63777	−0.18294
$Cl^{(2)}$	$\Phi_{xx}^{(2)}$	−0.07948	−0.45988	+0.88441
	$\Phi_{yy}^{(2)}$	+0.72295	+0.58426	+0.36877
	$\Phi_{zz}^{(2)}$	−0.68632	+0.66869	+0.28604
$Cl^{(3)}$	$\Phi_{xx}^{(3)}$	−0.06080	−0.32789	+0.90178
	$\Phi_{yy}^{(3)}$	+0.37378	−0.84748	−0.37691
	$\Phi_{zz}^{(3)}$	+0.92553	+0.31415	+0.21146
bond $C^{(i)}-Cl^{(j)}$				
$C^{(2)}-Cl^{(1)}$		+0.74959	−0.63691	−0.18018
$C^{(3)}-Cl^{(2)}$		−0.70731	+0.65302	+0.27071
$C^{(3)}-Cl^{(3)}$		+0.92884	+0.30435	+0.21121

Table 3. Best planes through the carbon-chlorine skeleton x'', y'', z'' are the positions of the atoms in the orthogonal system XYZ.

Plane I, $(C^{(1)}\,C^{(2)}\,C^{(3)}\,Cl^{(1)}\,Cl^{(2)}\,Cl^{(3)})$:
$-0.91306\,x''-0.41736\,y''+0.90414\,z''=-1.1778.$

Plane II, $(C^{(2)}\,C^{(3)}\,C^{(1)}\,Cl^{(2)}\,Cl^{(3)})$:
$-0.06641\,x''-0.40472\,y''+0.91203\,z''=-0.9790.$

Distances d/pm of the atoms from the planes.

Atom	Plane I, d/pm	Plane II, d/pm
$Cl^{(1)}$	5.4	3.5
$Cl^{(2)}$	5.3	3.1
$Cl^{(3)}$	−4.5	−0.6
$C^{(1)}$	−4.8	−12.6
$C^{(2)}$	−0.5	−4.0
$C^{(3)}$	−1.0	−2.0

Twisting of the carbonyl group $(O^{(1)}\,C^{(1)}\,O^{(2)})$:
$\measuredangle$ (plane $(O^{(1)}\,C^{(1)}\,O^{(2)})$, plane I) $=23.6°$
$\measuredangle$ (plane $(O^{(1)}\,C^{(1)}\,O^{(2)})$, plane II) $=23.6°$

Table 4. Bond lengths d and interpolated values for the asymmetry parameters $\eta(^{35}Cl)$, ^{35}Cl-NQR frequencies ν, and $eQ\Phi_{zz}h^{-1}(^{35}Cl)$ at 297 K.

Bond	d/pm	$\eta(^{35}Cl)$	ν/MHz	$eQ\Phi_{zz}h^{-1}$/MHz
$C^{(2)}-Cl^{(1)}$	172.4	0.1552	37.763	75.224
$C^{(3)}-Cl^{(2)}$	170.1	0.1607	38.289	76.251
$C^{(3)}-Cl^{(3)}$	170.6	0.1691	37.553	74.750

Table 5. Angles between the principal axes Φ_{ii}, $i=x,z$, of the EFG tensors and elements of the crystal structure (bond directions, normal $\boldsymbol{n}$ to the planes through atoms, etc.).

	$T=275$ K	$T=303$ K
$\measuredangle(\Phi_{zz}^{(1)}, Cl^{(1)}-C^{(2)})$	0.46°	0.25°
$\measuredangle(\Phi_{zz}^{(2)}, Cl^{(2)}-C^{(3)})$	1.89°	1.73°
$\measuredangle(\Phi_{zz}^{(3)}, Cl^{(3)}-C^{(3)})$	0.76°	0.56°
$\measuredangle(C^{(2)}-Cl^{(1)}, C^{(3)}-Cl^{(3)})$	62.33°	
$\measuredangle(\Phi_{zz}^{(1)}, \Phi_{zz}^{(3)})$	63.01°	63.03°
$\measuredangle(C^{(3)}-Cl^{(2)}, C^{(3)}-Cl^{(3)})$	113.66°	
$\measuredangle(\Phi_{zz}^{(2)}, \Phi_{zz}^{(3)})$	111.23°	111.37°
$\measuredangle(\Phi_{xx}^{(1)}, n(\text{plane}(Cl^{(1)}, C^{(2)}, C^{(3)})))$	−2.85°	−2.39°
$\measuredangle(\Phi_{xx}^{(2)}, n(\text{plane}(Cl^{(2)}, C^{(2)}, C^{(3)})))$	−4.87°	−3.11°
$\measuredangle(\Phi_{xx}^{(3)}, n(\text{plane}(Cl^{(3)}, C^{(2)}, C^{(3)})))$	−2.27°	−0.74°

directions C−Cl and Φ_{zz}-directions is (in the drawing) within the limits of error, see Table 5.

Looking more carefully at the angles given in Table 5, one finds the following:

a) There is a narrowing of the angle $(\Phi_{zz}^{(2)}, \Phi_{zz}^{(3)})$ compared to the corresponding bond angle $(Cl^{(2)}-C^{(3)}-Cl^{(3)})$; the former angle is 111.2°, the latter one 113.7°. In all the systems incorporating a planar carbon skeleton with (partial) double bond character, such as benzene derivatives, we observed a widening of the angles the ^{35}Cl-EFGT's form in comparison with the bond angles. Compared with aromatic sys-

tems and considering the fact that in $Cl_2C=CClCOOH$ the atoms $Cl^{(2)}$ and $Cl^{(3)}$ are bound to the same carbon atom $C^{(3)}$, the narrowing of the angle in trichloroacrylic acid is strong (the distance $Cl^{(2)} \cdots Cl^{(3)}$ within one group $=CCl_2$ is 285.2 pm, considerably below the van der Waals distance for two chlorine atoms). For example, in 1,2,3-trichlorobenzene [4] the angles between the bond directions, $\measuredangle(Cl^{(1)}-Cl^{(1)}, C^{(2)}-Cl^{(2)})$ and $\measuredangle(C^{(2)}-Cl^{(2)}, C^{(3)}-Cl^{(3)})$, are 61.04° and 60.71°, whereas the corresponding angles $\measuredangle(\Phi_{zz}, \Phi_{zz})$ are 62.0° and 62.17°, respectively. It seems that the widening of the EFGT angles in resonant systems by mutual polarisation of the Cl-atoms is not found in a true sp^2-system. The observation is in agreement with another result of our Zeeman split NQR investigations: If the structure shows a reasonable deviation from the ideal bond angle, this deviation is always even larger concerning the corresponding $\measuredangle(\Phi_{zz}, \Phi_{zz})$. Here the "ideal bond angle" would be 120°. The structure shows a deviation to a smaller angle, and for the Φ_{zz}'s this tendency is increased.

b) There is another interesting observation for the EFGT's of ^{35}Cl in trichloroacrylic acid. The ^{35}Cl-NQR frequencies of the stereochemically inequivalent chlorines $Cl^{(2)}$ and $Cl^{(3)}$ differ considerably, as do the corresponding $eQ\Phi_{zz}h^{-1}$ (^{35}Cl). While $Cl^{(2)}$ is located trans to the pi-electron-donating $Cl^{(2)}$, $Cl^{(3)}$ is located trans to the pi-electron-accepting COOH group. The resulting electronic differences, as well as crystal field effects, may produce the fairly large differences of $eQ\Phi_{zz}h^{-1}$ (^{35}Cl) of $Cl^{(2)}$ and $Cl^{(3)}$.

c) A further interesting outcome of the single crystal Zeeman NQR in $Cl_2C=CClCOOH$ is the temperature behavior of η (^{35}Cl), see Table 1. $Cl^{(2)}$ and $Cl^{(3)}$ show in ^{35}Cl-NQR the "normal" temperature dependence one expects, and which we have observed in the studies of several compounds. The EFGT of $Cl^{(1)}$, however, shows an increase of η (^{35}Cl) with increasing temperature (barely above the limits of error). Nevertheless, compared to $Cl^{(2)}$ and $Cl^{(3)}$, the temperature dependence of η (^{35}Cl) of the EFGT ($Cl^{(1)}$) is different from that of the chlorines in the $=CCl_2$ group. This may well be due to the phase transition, connected with a "switching" of the hydrogens in the dimeric unit into fixed positions within the molecule $(Cl_2C=CClCOOH)_2$.

We are grateful to the Stiftung Volkswagenwerk for support of this work. One of us, G. W., is thankful to the Alexander von Humboldt-foundation for a fellowship.

[1] S. Fleck, R. Göckel, and Al. Weiss, J. Mol. Struct. **161,** 139 (1987).
[2] V. Nagarajan, N. Weiden, R. Wendel, and Al. Weiss, J. Magn. Reson. **47,** 28 (1982).
[3] A. Markworth, N. Weiden, and Al. Weiss, Ber. Bunsenges. Phys. Chem. **91,** 1158 (1987).
[4] S. Sharma, N. Weiden, and Al. Weiss, Ber. Bunsenges. Phys. Chem. **90,** 725 (1986).